Utilizing Swelling Force to Decrease the Ice Adhesion Strength

Tingkun Chen[1], Qian Cong[1,2], Yang Li[1], Jingfu Jin[1※], Kwang-Leong Choy[3]

1. Key Laboratory of Bionic Engineering, Ministry of Education, Jilin University, Changchun 130022, P.R.China.

2. State Key Laboratory of Automotive Simulation and Control, Jilin University, Changchun 130022, P.R.China.

3. Institute for Materials Discovery, University College London, London WC1E 7JE, United Kingdom.

Abstract

The phase transformation that occurs during water freezing process is accompanied by volume expansion and the release of latent heat. The swelling force generated by this phase transformation can have a harmful impact on structural safety and integrity, as it can lead to bursting in roads, water pipes and reservoir dams. So, why not effectively adopt the swelling force as the active de-icing power to diminish the stability of the contact interface. This paper proposes a new method to remove this accumulated ice by using polymethyl methacrylate (pmma) and 6061 aluminum alloy with pits as substrate materials. Pits were filled with solutions of different freezing points; owing to the different freezing point between the pit solution and water, their phase transformations occurred at different time, where the solutions in the pit would freeze more slowly than the surface water. The generated phase swelling force directly acted on the contact interface and decreased the stability of the interface to decrease the

Corresponding author: Jingfu Jin
Corresponding author at: 5988 Renmin Street, Changchun, 130025, China
E-mail: jinjingfu@jlu.edu.cn
Fax number: +86-431-85095575-888

ice adhesion strength. The experimental results showed that the ice adhesion strength was obviously affected and reduced by the swelling force in contrast to the ice adhesion strength on the smooth sample, and the reduction in ice adhesion strength changed depending on the filling solution. Compared to the ice adhesion strength of the specimen without pits, the frozen ice was completely separated from the ice-pmma interface owing to the water filling the pit. The ice adhesion strength on the surface of the aluminum alloy sample filled with 10% ethanol solution was reduced by 81.42%. Utilizing the phase swelling force to reduce the adhesion strength enhances the active de-icing ability of the material, providing a novel method for developing new anti-icing methods.

Keywords: De-icing; Phase transformation; Swelling force; Phase change time difference; Ice adhesion strength; Contact interface

1. Introduction

Ice adhesion on exposed surfaces is considered as a potential hazard in many engineering fields including in aircraft, wind turbines, power lines, high speed trains and other industrial areas (Bewilogua et al., 2009; Carriveau et al., 2012; Cucchiella et al., 2012; Caliskan et al., 2013; Zhang et al., 2015). It is well known that ice adhesion can also degrade the operational reliability and durability of equipment, even posing a great hazard to people's lives and causing the socio-economic loss. Serious examples include the 2008 ice storm in southern China, and the 1998 ice storm in northeast North America (Ruan et al., 2016; Petrenko et al., 2011; Stone et al., 2008).

Conditions such as these have prompted researchers and engineers to develop practical and economical anti-icing or de-icing methods. More than 30 kinds of de-icing methods have been formed in the pursuit of materials with excellent ice-phobic properties, which can be classified in three function categories: heating, mechanical scraping and chemical agents. While these methods are widely used in engineering, many shortcomings still exist, in terms of energy consumption, environmental impact and cost (Parent et al., 2011; Koenig et al., 2011; Makkonen et al., 2012).

Since the discovery of superhydrophobic surfaces represented by the lotus leaf phenomenon and recent developments in materials fabrication, an appealing method for mitigating ice adhesion is to use icephobic coatings to repel ice or reduce ice adhesion on an exposed surface (Zheng et al., 2017). Superhydrophobic surfaces are regarded as a promising way to remove accumulated ice because of their extraordinary water-repellency. Therefore, it is no surprise that recent research in this field has focused predominantly on the use and development of superhydrophobic surfaces. To demonstrate the dual role in delaying nucleation played by superhydrophobic surfaces, Alizadeh et al (2012) utilized infrared thermometry and high-speed photography to measure and observe the freezing process of droplets on superhydrophobic surfaces. However, recent literatures on how hyrdrophobic and superhydrophobic surfaces can reduce ice adhesion strength or repel water have featured poor durability (Kulinich and Farzaneh, 2009, 2011; Lazauskas et al., 2013). Meanwhile, many shortcomings have appeared during actual use, such as poor pollution resistance, high preparation cost and other disadvantages (Karmouch et al., 2010; Varanasi et al., 2010; Jung et al., 2011;

Kulinich et al., 2011). Despite numerous efforts to mitigate these problems, a simple, effective and inexpensive anti-icing technique has yet to be found.

A phase transformation must occur when water freezes and this freezing is accompanied by a volume increase and the generation of an expansive force. This force has an impacted on engineering structures in cold regions, such as reservoirs, marine structures, breakwaters and retaining walls (Healy et al., 2006; She et al., 2006; Iliescu et al., 2007). For instance, when the South-to-North Water Diversion crosses into cold regions, the expansive load generated by icing acts on the ditch, greatly impacting its performance and operational safety (Fu et al., 2015).

If this swelling force could be harnessed in a reasonable and effective manner, it could become a useful anti-icing or de-icing solution. In cold settings, water or moisture attached to a material surface would be frozen into the ice, and the stability of the ice-substrate surface greatly influences the ice adhesion. Hence, this work proposes a new de-icing model: ones that takes the phase swelling force as the active power to impact the stability of the contact surface in order to reduce the ice adhesion strength, and making it very easy to remove accumulated ice.

2. Materials and methods

2.1 Anti-icing model and theory

This study puts forward an active de-icing model that uses the expansive force to remove accumulating ice, as shown in Fig. 1. The substrate has a pit filled with water or solutions that have a lower freezing point than water (0 ℃). Therefore, there is a difference in phase transition time between the water and the media located in the pit. The surface of the material is covered by an elastic film. At low temperatures, water or moisture attaches to the film in an adhesive manner, which freezes first and becomes attached to the surface of the material. Owing to the thermal conductivity and the lower freezing point, the solution under the membrane begins to freeze later than the water attached to the membrane.

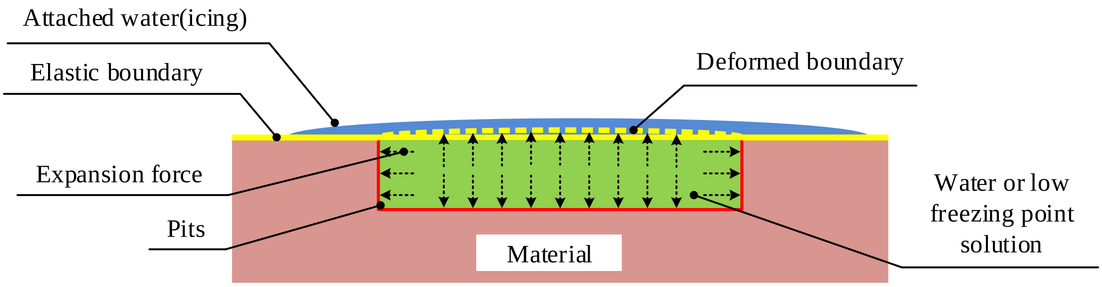

Fig 1. Schematic of the proposed anti-icing model

During the freezing process, the solution undergoes the stage of volume expansion and freezes into a pointy ice-drop (Peters et al., 2009; Enríquez et al., 2012; Snoeijer et al., 2012; Chaudhary et al., 2014). The size changes significantly after freezing into ice compared to the height of the water droplets, as shown in Fig. 2 where, H is significantly larger than h. Therefore, the swelled load generated by the freezing solution filling the pit would directly act on the elastic film and causes deformation. This would result in the contact interface becoming defective, affecting the contact stability of the interface between the material and ice. The ice adhesion strength would therefore decrease, making the accumulation ice easy to remove.

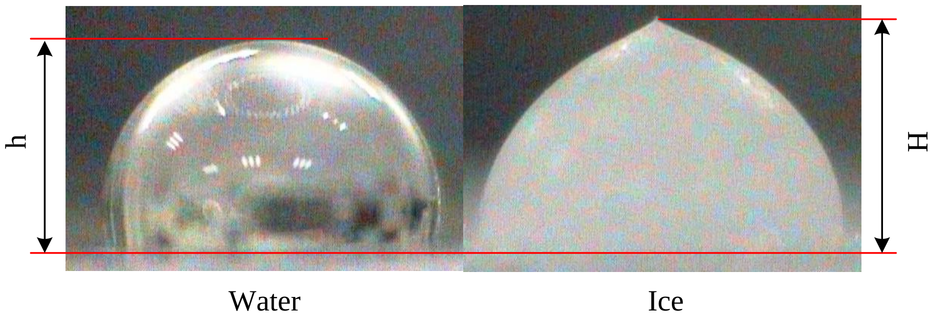

Fig 2. Droplet shapes after freezing

2.2 Materials

To demonstrate the effectiveness of this de-icing model, experiments were performed using a cup method to fabricate ice for testing, as shown in Fig. 3. In order to eliminate the influence of thermal conductivity on this anti-icing model, our tests employed 6061 aluminum alloy and polymethyl methacrylate (pmma) with thermal conductivities of 237 W/m·k and 0.2 W/m·k respectively, to represent materials with good and poor thermal conductivities. All samples were 60 mm×60 mm×6 mm (L×W×H) in size, and the specimens with the pits were covered by a biaxially oriented polypropylene (bopp) film as the elastic contact interface. The pits were machined using a milling method, where pits 30 mm in diameter and 3.5 mm deep, were filled with water or other lower freezing point solutions such as the ethanol solution, glycol solution, glycerine solution.

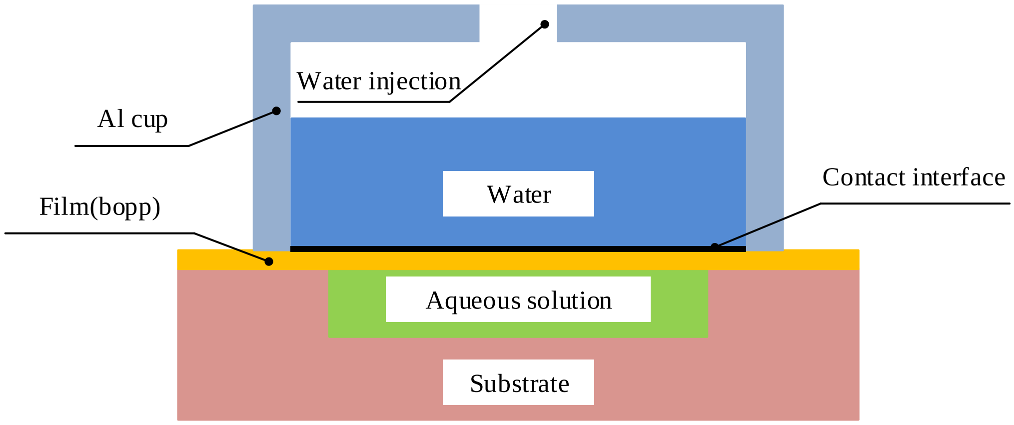

Fig 3. Schematic of the anti-icing model

2.3 Characterization of the frozen medium

In addition to being filled with water, the pits could be filled with different mass concentrations of ethanol solution and glycol solution during different experiments; ethanol solutions and glycol solutions with mass concentrations of 10%, 15%, 20% were used. The differences in freezing temperature between water and the different solutions are shown in Table 1.

Table 1 Freezing points of test solutions (ºC)

Mass concentration	Ethanol solution	Glycol solution
10%	-4.7	-3.5
15%	-6.8	-5.3
20%	-10.4	-8.8

The temperature change curves were recorded during the freezing process of these aqueous solutions under the same ambient temperature. The temperature of the liquid was measured by a K-type thermocouple embedded in the sample pit, having an accuracy of ±1.0%.

2.4 Experimental conditions

During the experiments, the entire anti-icing model was placed in a climate chamber controlled to an ambient temperature at -25 ^{o}C and was frozen for 1 h, the temperature accuracy of the climate chamber was ±0.01 ^{o}.. The phenomenon of ice adhesion could be regarded as ice, a special adhesive, attaching to the material surface under low temperature conditions. Therefore, the test device was designed according to the ASTM-D3528 (2008) standard, as shown in Fig. 4. The experiment adopted the more intuitive and simple unit N to evaluate the shear ice adhesion strength. The inner diameter of the aluminum cup was 32 mm.

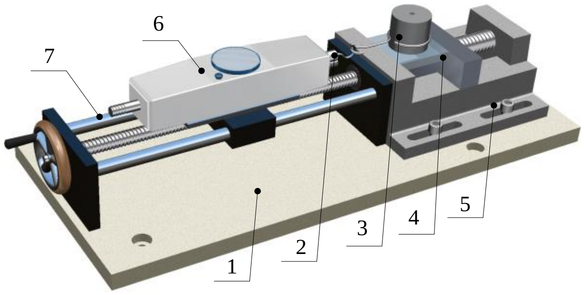

1. Base; 2. Connecting ring; 3. Aluminum alloy cup; 4.Sample; 5. Vice;

6. Draft gauge; 7. Rally stand.

Fig 4. Ice adhesion strength test device

The accumulated ice was peeled off from the material surface by pushing the draft gauge, and the maximum force was recorded during the peeling process. In this paper, the ice adhesion force is defined as the tangential ice adhesion strength because it can be easily compared to the results of other works. The precision of the draft gauge is 0.1 N.

3. Results

3.1 Ice adhesion strength

Pits of aluminum alloy and pmma were filled with water and different mass concentrations of ethanol and glycol solutions, and the ice adhesion strength on the smooth sample (without pits) was tested as a reference. The samples were labeled as *A, B, C, D, E, F, G, H,* and the characteristics of each sample are shown in Table 2.

Table 2 Sample descriptions

Medium	None (without pit)	Water	Ethanol solution			Glycol solution		
			10%	15%	20%	10%	15%	20%
Name	A	B	C	D	E	F	G	H

Eight different samples were tested twenty times each, and the average results was taken as the ice adhesion strength of the sample in question. Fig. 5 summarizes the experimental results.

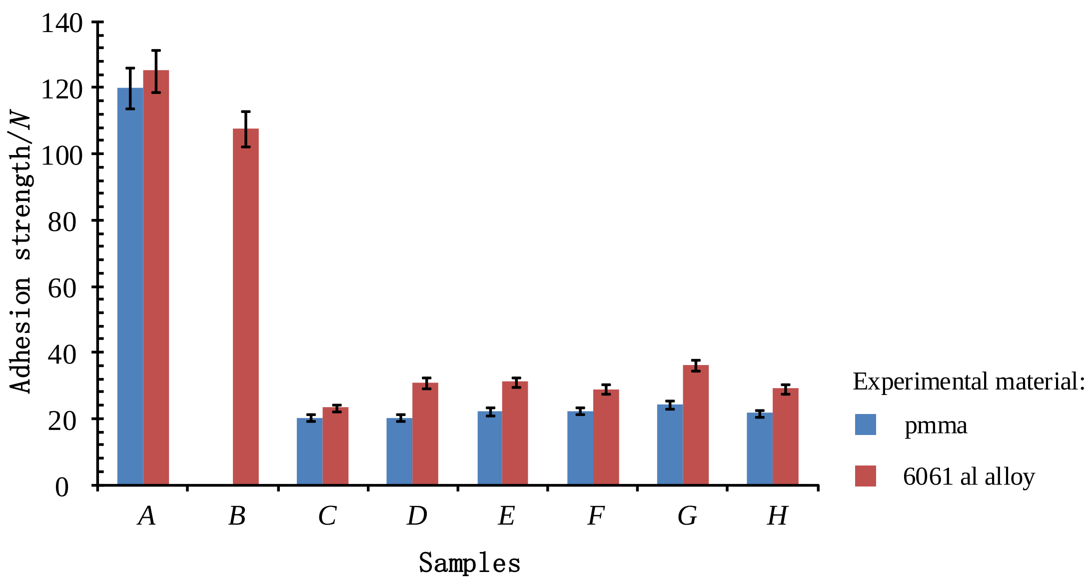

Fig 5. Shear ice adhesion strength. 1)Adhesion strength on the B_{pmma} sample was 0 N. 2)*A*-smooth sample; *B*-the pit of sample filled with water; *C*, *D*, *E*- the sample pit full of 10%, 15%, 20% mass concentration of ethanol solution, respectively; *F*, *G*, *H*- full of 10%, 15%, 20% mass concentration of glycol solution, respectively.

The adhesion strengths of samples with the solution-filled pits were substantially lower than that in smooth specimen; in particular, the ice adhesion strength of sample B_{pmma} was 0 N, with a 100% reduction rate. The ice adhesion strength of $B_{6061\ al}$ which had formed with 107.74 N, was obviously larger than that of $C_{6061\ al}$-$H_{6061\ al}$. The ice adhesion strength of the aluminum alloy specimens was obviously larger than in the case of the pmma surfaces. No matter whether the pit filled with ethanol solution or glycol solution, the ice adhesion strength on the aluminum alloy and pmma had similar growth trends. When the pits were filled with ethanol solution, the ice adhesion strength increased gradually with increasing mass concentration in the ethanol solution, while the growth rate gradually decreased with this trend. In addition, ice adhesion strength of the samples containing of glycol solutions first increased and then diminished with increasing in mass concentration. For example, the ice adhesion strength of aluminum alloy samples with different mass concentrations of ethanol solution were 23.25 N, 30.85 N, and 31.1 N, respectively, and the strengths of samples $F_{6061\ al}$-$H_{6061\ al}$ were 28.86 N, 36.2 N, and 29.17 N, respectively.

3.2 Surface topography after testing

Owing to the elasticity of the attached film, the swelling load generated by freezing of the different solutions in the pits can act on the surface, such that the contact surface could produce different surface morphologies. Fig. 6 shows the surface topography after the ice adhesion strength tests.

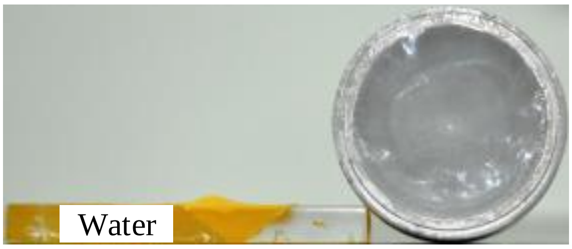

Fig 6. Surface topography of pmma specimen filled with water after freezing and peeling the accumulated ice

The morphology of the freezing interface obviously changed, and the area of the pit featured irregular deformation because the solution froze and underwent the volume expansion. The membrane of the sample with water in the pit generated the largest expansive deformation, as shown in Fig. 6.

3.3 Freezing characteristics of the solution

The purpose of using the phase change time differential between the two kinds of freezing media was to adopt the swelling force and to reduce the ice adhesion strength. Therefore, it is necessary to understand the temperature variation during freezing process. Under similar conditions, the temperatures of several kinds of solutions adopted in the ice adhesion strength tests and water attached on the covered film were measured. Taking the 10% mass concentration of ethanol solution as an example, the curves of the change in temperature of the solution in the pits and water were recorded using a thermal conductor (± 0.01 ^{o}C)and are shown in Fig. 7.

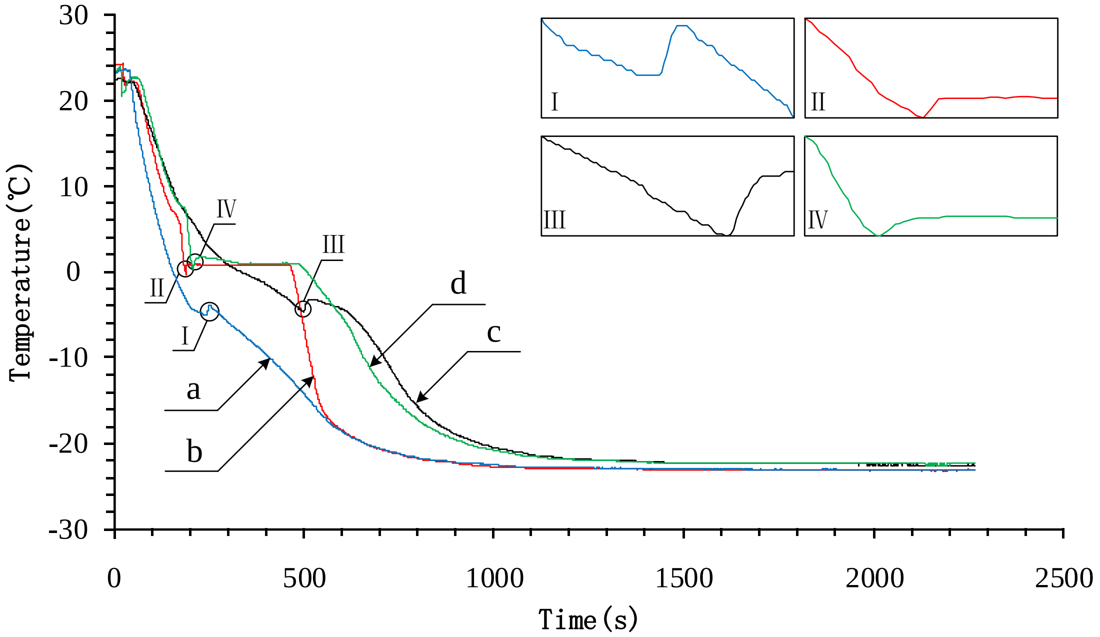

Fig 7. Changes in solution temperature during the freezing process: (a) temperature curve of solution in pit of 6061 aluminum alloy; (b) temperature curve of water attached on 6061 aluminum alloy; (c) temperature curve of solution in pit of pmma; (d) temperature curve of water attached on pmma.

As shown in Fig. 7, the freezing times of the media in the pits were later than those of the water attached on the membrane surfaces. This was especially apparent for pmma with its poor thermal conductivity, where a large time difference between two kinds of media in the freezing time was observed.

During the freezing process, the temperature variations of both the solution in pits and the water attached to the film were measured, and the differences in the phase transition behavior of the two media are given in Table 3.

Table 3 Phase transition time differences between water and pit solutions (s)

Materials / Solution	6061 Aluminum alloy	Polymethyl methacrylate (pmma)

Water	43	306.67
10% Ethanol solution	141	502.33
15% Ethanol solution	285.75	760.75
20% Ethanol solution	520.75	971
10% Glycol solution	95.33	465
15% Glycol solution	195	642.67
20% Glycol solution	305.33	878.75

As the mass concentration increases, the difference in phase transformation time between the water and test solution increases in magnitude. At the same time, the thermal conductivity of the sample would also affect the phase transition time differently between water and the test solutions.

4. Discussion

Based on the experimental results, this anti-icing model is effective for reducing the ice adhesion strength. In this setup, the swelling force associate with the phase change would destroy the freezing interface, and have a great influence on decreasing the ice adhesion strength. By comparing the freezing strengths on 6061 aluminum alloy and pmma (representing materials with good and poor thermal conductivity respectively), the thermal conductivity of the freezing substrate has a minimal influence on the anti-icing model, in terms of reducing the ice adhesion strength.

Owing to the thermal conductivity and freezing point of the liquid in the pits, there was a difference in the order of freezing between the water attached on the film and the medium located in the pits. At -25 ^{o}C, water above the membrane begin to freeze, forming a stable and smooth contact interface. By prolonging the freezing time, the medium in the pits begins to undergo phase change, and the latent heat of the phase transformation was released during the process, of which the expansion force is one forms. During the freezing process, we assumed that the phase transformation expansion of the lower freezing point solution was caused primarily by the water component in solution, regardless of the molecular interactions between ethanol/ glycol and water. Therefore, the latent heat of solidification in these lower freezing point solutions filled was equal to the energy released by freezing the water component of the solution. The theoretical calculated values for the latent heat of solidification of each solution are given in Table 4.

Table 4 Theoretical solidification latent heats of sample solutions (*kJ/L*)

Medium	Water	Ethanol solution			Glycol solution		
		10%	15%	20%	10%	15%	20%
Latent heat	334.39	295.50	277.18	259.11	311.18	296.34	281.05

The freezing process of the aqueous solution was quick and released a high amount of energy, as shown in Fig. 7 and Table 4, and volume expansion occurred. The solution in the pit underwent a rapid phase change and release of expansive energy akin to an explosion, leading to a very high energy density. Since the sides of the pit were covered by an elastic boundary, the released expansion energy only acted on the elastic film causing film deformation, and turning the stable and smooth interface into a rugged one, as shown in Fig. 8.

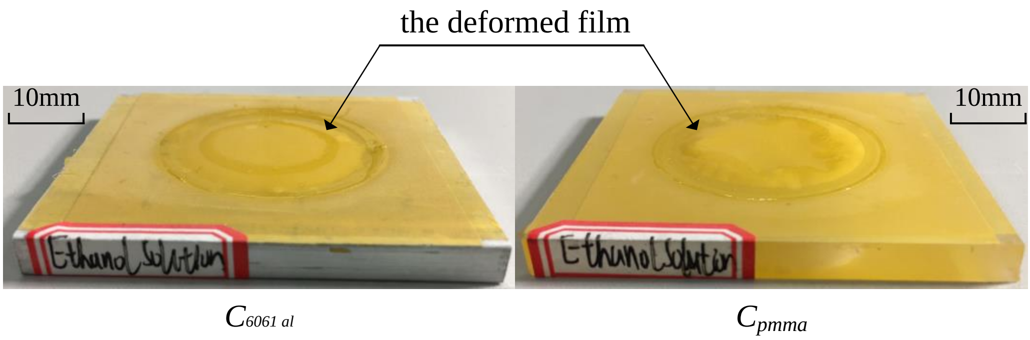

Fig 8. Deformed elastic membranes

Of all tested specimens, the freezing strength of B_{pmma} filled with water in the pit was the lowest, at 0 N. However, the ice adhesion strength of $B_{6061\ \mathrm{al}}$ was slightly lower than that of the smooth aluminum specimen, which was higher than that of the other samples. Since the phase difference of sample $B_{6061\ \mathrm{al}}$ was less than in any other sample, the attached water was frozen first. Shortly, after the above surface water froze, the medium located in the pit began to freeze along with a volume expansion that caused deformation in the elastic film. The anti-icing model continued to be refrigerated in the climate chamber, and the interface between the deformed membrane and the ice would be reformed. Although the ice adhesion strength on the reformed interface was reduced, the reduction rate was small. The interface of $B_{6061\ \mathrm{al}}$ still had a small amount of ice slag after peeling off the ice, but the surface of B_{pmma} free of ice residue and water in the pit where the volume expansion occurred, and the ice attached on the surface had completely peeled off.

When the pit is filled with liquid having a lower freezing point than water, there is a difference in phase transition time between the test liquid and water. This causes volume expansion and the release of swelling energy by freezing the solution, to deform the elastic boundary, and destroy the contact stability and continuity. Thus, the freezing strength is reduced.

5. Conclusions

In summary, the ice on the polymethyl methacrylate (pmma) substrates having pits filled with water were thoroughly separated from the sample surface, and the ice adhesion strength of B_{pmma} was the smallest, 0 N. Different kinds of solutions had different effects on the ice adhesion strength reduction rate based on material type, but the ice adhesion strength on different samples with pit were remarkably reduced compared to those on samples without pits.

The proposed de-icing model achieved a good de-icing effect and reduced the ice adhesion strength in experimental studies. It was found that the influence of the substrate's thermal conductivity was small. During the de-icing model, pits on the substrates were filled with water or other solutions with lower freezing points compared to water. Because of this, there was a phase transition time difference during the de-icing models. In the cold surroundings, the water is firstly frozen the ice owing to the thermal conductivity of the material itself. When the solution in the pit began to solidify, it underwent expansion associated with this phase transformation. The swelling force generated in a short time acted on the elastic contact interface to cause film deformation. Furthermore, this destroys the stability of the interface between the ice and the sample surface. Thus, the ice adhesion strength could be reduced and the aim of de-icing would be achieved.

Based on the experiment results, this paper provides a novel method for developing anti-icing methods at low cost, with high de-icing efficiency and minimal pollution, and we get an inspiration, such as the fabrication of the microscopic structure to contain the solution, or similar to the honeycomb structure attached on the material to improve the active de-icing performance of substrate.

Acknowledgments

This study was financially supported by the International Exchanges Scheme Between the Royal Society and the NSFC (grant number. 51711530236).

References

ASTM D3528-96(2008). Standard test and method for strength properties of double lap shear adhesive joints by tension loading [S].

Alizadeh, A., Yamada, M., Li, R., et al, 2012. Dynamics of ice nucleation on water repellent surfaces. Langmuir 28(6), 3180-3186.

Bewilogua, K., Bräuer, G., Dietz, A., et al, 2009. Surface technology for automotive engineering. CIRP Annals – Manuf. Technol. 58(2), 608-627.

Carriveau, R., Edrisy, A., Cadieux, P., et al, 2012. Ice adhesion issues in renewable energy infrastructure. J. Adhes. Sci. Technol. 26(4-5), 447-461.

Cucchiella, F., D'Adamo, I., 2012. Estimation of the energetic and environmental impacts of a roof-mounted building-integrated photovoltaic systems. Renew. Sustain. Energy. Rev. 16(7), 5245-5259.

Caliskan, F., Hajiyev, C., 2013. A review of in-flight detection and identification of aircraft icing and reconfigurable control. Prog. Aerosp. Sci. 60, 12-34.

Chaudhary G., Li, R., 2014. Freezing of water droplets on solid surfaces: An experimental and numerical study. Exp. Therm. Fluid Sci. 57, 86-93.

Enríquez, O.R., Maríın, Á.G., Winkels, K.G., 2012. Freezing singularities in water drops. Phys. Fluids. 24(9), No. 091102.

Fu, H., Yang, K., Guo, X.L., et al, 2015. Safe operation of inverted siphon during ice period. J. Hydrodyn. 27(2), 204-209.

Healy, D., Hicks, F.E., 2006. Experimental study of ice jam formation dynamics. J. Cold Reg. Eng. 20(4), 117-139.

Iliescu, D., Bake, I., 2007. The structure and mechanical properties of river and lake ice. Cold Reg. Sci. Technol. 48(3), 202-217.

Jung, S., Dorrestijn, M., Raps, D., et al, 2011. Are superhydrophobic surfaces best for icephobicity?. Langmuir, 27(6), 3059-3066.

Koenig, G.G., Ryerson, C.C., 2011. An investigation of infrared deicing through experimentation. Cold Reg. Sci. Technol. 65(1), 79-87.

Karmouch, R., Ross, G.G., 2010. Experimental study on the evolution of contact angles with temperature near the freezing point. J. Phys. Chem. C. 114(9), 4063–4066.

Kulinich, S.A., Farzaneh, M., 2009. How wetting hysteresis influences ice adhesion strength on superhydrophobic surfaces. Langmuir, 25(16), 8854-8856.

Kulinich, S.A., Farhadi, S., Nose, K., et al, 2011. Superhydrophobic surfaces: are they really ice-repellent?. Langmuir, 27(1), 25-29.

Kulinich, S.A., Farzaneh, M., 2011. On ice-releasing properties of rough hydrophobic coatings. Cold Reg. Sci. Technol. 65(1), 60-64.

Lazauskas, A., Guobiene, A., Prosyčevas, I., et al, 2013. Water droplet behavior on superhydrophobic SiO_2 nanocomposite films during icing/deicing cycles. Mater. Charact. 82, 9-16.

Makkonen, L., 2012. Ice adhesion —theory, measurements and countermeasures. J. Adhes. Sci. Technol. 26(4-5), 413-445.

Peters, I., Snoeijer, J.H., Daerr, A., et al, 2009. Coexistence of two singularities in dewetting flows regularizing the corner tip. Phy. Rev. Lett. 103(11), No. 114501.

Parent, O., Ilinca, A., 2011. Anti-icing and de-icing techniques for wind turbines: Critical review. Cold Reg. Sci. Technol. 65(1), 88-96.

Petrenko, V.F., Sullivan, C.R., Kozlyuk, V., 2011. Variable-resistance conductors (VRC) for power-line de-icing. Cold Reg. Sci. Technol. 65(1), 23-28.

Ruan, M., Wang, J.W., Liu, Q.L., et al, 2016. Superhydrophobic and anti-icing properties of sol-gel prepared alumina coatings. Russian J. Non-Ferr. Met. 57(6), 638-645.

Snoeijer, J.H., Brunet, P., 2012. Pointy ice-drops: How water freezes into a singular shape. Am. J. Phy. 80(9), 764-771.

Stone, R., 2008. Natural disasters. Ecologists report huge storm losses in China's forests. Science 319(5868), 1318-1319.

She, Y., Hicks, F., 2006. Modeling ice jam release waves with consideration for ice effects. Cold Reg. Sci. Technol. 45(3), 137-147.

Varanasi, K.K., Deng, T., Smith, J.D., et al, 2010. Frost formation and ice adhesion on superhydrophobic surfaces. Appl. Phys. Lett. 97(23), No. 234102.

Zheng, H.K., Chang, S.N, Zhao, Y.Y, 2017. Anti-icing & icephobic mechanism and applications of superhydrophobic/ultra slippery surface. Prog. Chem. 29(1), 102-118.

Zhang, P, Lv, F.Y, 2015. A review of the recent advances in superhydrophobic surfaces and the emerging energy-related applications. Energy 82, 1068-1087.